A meta-analysis of brain DNA methylation across sex, age and Alzheimer's disease points for accelerated epigenetic aging in neurodegeneration

Pellegrini C[1], Pirazzini C[1], Sala C[2], Sambati L[1,3], Yusipov I[4], Kalyakulina A[4], Ravaioli F[5], Kwiatkowska KM[5], Durso DF[6], Ivanchencko M[4], Monti D[7], Lodi R[1,3], Franceschi C[4], Cortelli P[1,3], Garagnani P[5,8,9,10], Bacalini MG[1]*

1 IRCCS Istituto delle Scienze Neurologiche di Bologna, Bologna, Italia.
2 Department of Physics and Astronomy, University of Bologna, Bologna, Italy.
3 Department of Biomedical and Neuromotor Sciences, University of Bologna, Bologna, Italy.
4 Institute of Information Technologies, Mathematics and Mechanics, Lobachevsky University, Nizhniy Novgorod, Russia
5 Department of Experimental, Diagnostic and Specialty Medicine, University of Bologna, Bologna, Italy.
6 Department of Neurology, University of Massachusetts Medical School, Worcester, Massachusetts, United States of America
7 Department of Experimental and Clinical Biomedical Sciences "Mario Serio", University of Florence, Florence, Italy.
8 Department of Laboratory Medicine, Clinical Chemistry, KarolinskaInstitutet, Karolinska University Hospital, Stockholm, Sweden.
9 Applied Biomedical Research Center (CRBA), Policlinico S.Orsola-MalpighiPolyclinic, Bologna, Italy.
10 CNR Institute of Molecular Genetics "Luigi Luca Cavalli-Sforza", Unit of Bologna, Bologna, Italy.

*Correspondence:
Maria Giulia Bacalini
mariagiulia.bacalini@ausl.bologna.it

Abstract

Alzheimer's disease (AD) is characterized by specific alterations of brain DNA methylation (DNAm) patterns. Age and sex, two major risk factors for AD, are also known to largely affect the epigenetic profiles in the brain, but their contribution to AD-associated DNAm changes has been poorly investigated. In this study we considered publicly available DNAm datasets of 4 brain regions (temporal, frontal, entorhinal cortex and cerebellum) from healthy adult subjects and AD patients, and performed a meta-analysis to identify sex-, age- and AD-associated epigenetic profiles. We showed that DNAm differences between males and females tend to be shared between the 4 brain regions, while aging differently affects cortical regions compared to cerebellum. We found that the proportion of sex-dependent probes whose methylation changes also during aging is higher than expected, but that differences between males and females tend to be maintained, with only few probes showing sex-by-age interaction. We did not find significant overlaps between AD- and sex-associated probes, nor disease-by-sex interaction effects. On the contrary, we found that AD-related epigenetic modifications are significantly enriched in probes whose DNAm changes with age and that there is a high concordance between the direction of changes (hyper or hypo-methylation) in aging and AD, supporting accelerated epigenetic aging in the disease.

In conclusion, we demonstrated that age-associated, but not sex-associated DNAm concurs to the epigenetic deregulation observed in AD, providing new insight on how advanced age enables neurodegeneration.

KEYWORDS: Epigenetic modifications, DNA Methylation, Alzheimer's disease, Brain, Sex, Aging

INTRODUCTION

Alzheimer's disease (AD) is a chronic neurodegenerative disease that leads to a progressive decay of cognitive abilities and self-sufficiency. Neuronal loss involves multiple brain regions that are progressively affected by the disease. Hippocampus and entorhinal cortex exhibit the earliest pathological changes, preceding the onset of clinical signs and cognitive impairment by several years, and later the disease spreads to the other brain regions(1-4).

Advanced age and female sex are the two major non-modifiable risk factors for AD(5-7). More than 95% of cases of AD occur after 65 years of age (late onset AD, LOAD), and AD prevalence increases exponentially between 65 and 85 years (8, 9).Two-thirds of clinically diagnosed cases of AD are women, and the fact that women live longer than man does not fully explain this sex bias for AD (10, 11).

The etiology and pathogenesis of AD are complex and likely result from the interplay between genetic and environmental factors during lifespan. In this scenario epigenetic modifications have attracted increased interest in the study of AD, as they integrate genetic background and environment and modulate genomic organization and gene expression. Epigenetic modifications regulate brain biology throughout development and lifetime, influencing neuronal plasticity, cognition and behavior (12), and deregulation of brain epigenetic patterns has been correlated to the pathogenesis of neurological and psychiatric disorders (13, 14). Several studies in post-mortem brain have investigated the role of DNA methylation (DNAm), the best characterized epigenetic modification, in AD, identifying a number of CpG sites that show robust changes in DNAm compared to non-demented controls (15-24).

Interestingly, the two major non-modifiable AD risk factors mentioned above, *i.e.* sex and age, are also among the main biological variables that influence epigenetic patterns in most human tissues, including brain (25).

Genome-wide DNAm differences between males and females have been found in whole blood (26) and have been related to the sex-biased risk of psychiatric diseases (27). A similar link has been reported also in brain (28)where sex-specific DNAm patterns are established early during prenatal development (29, 30)and are at least in part maintained in the adulthood (29, 31), contributing to the profound differences in brain functions between males and females (32-34) and to the different onset of psychiatric disorders(30).

DNAm patterns are largely remodeled during aging (35), where a trend towards global loss of DNA methylation together with hypermethylation at specific loci is observed(36).Although with some differences between brain regions (37, 38), age-associated epigenetic changes interest also the brain, likely contributing to the structural and functional alterations that can resulting progressive cognitive decline and increased susceptibility to neurodegenerative disorders(39, 40).

So far, only few studies have considered how sex and age interact during lifespan in shaping the epigenome. Data on whole blood indicate that sex-dependent DNAm is remodeled during aging (41), and we suggested that these changes occur at different extent in human models of successful and unsuccessful aging. In mouse hippocampus and human frontal cortex, Masser et al identified CpGs in which sex-dependent DNAm is maintained lifelong and CpG sites that are differentially affected by aging in relation to sex (42). Interestingly, some studies employing epigenetic clocks, *i.e.* DNAm-based predictors of age, reported accelerated aging in whole blood from males compared to females (43-45), and the same trend was observed also in brain (43).

Collectively, the available data sustain the importance of sex and aging in shaping the brain epigenome, but so far only one study reported sex-associated DNAm differencesthat were reproducible in different datasets and brain regions (28). No study has systematically analyzed multiple datasets and brain regions to identify DNAm patterns resulting from the interaction of sex and age during lifespan, and most importantly no study has evaluated whether sex- and age-dependent DNAm can contribute to epigenetic deregulation in AD, despite the pivotal role of these two factors in AD etiology and pathogenesis.
To fill this gap, in the present study we performed a meta-analysis of DNAm across sex, age and AD considering publicly available datasets from different brain regions.

MATERIALS AND METHOD

Datasets

To select DNA methylation datasets based on Infinium BeadChip technology, the Gene Expression Omnibus (GEO) repository (46) was interrogated by the GEOmetadb Bioconductor package using the following search terms:“GPL13534”, “GPL21145”, to include only datasets based on the Illumina Infinium HumanMethylation450 and MethylationEPIC BeadChips; “sex”, “gender”, “female”, to include only datasets in which the information on the sex of the subjects was available; “age”, to include only datasets in which the information on the age of the subjects was available; “brain”, “cortex”, “gyrus”, “lobe”, “gray”, to select datasets in which brain samples were analysed; “control”, “normal”, “non-tumor”, “health”, or “Alzheiemer”, “AD”, “Braak”, to select datasets including healthy and AD subjects, respectively. We considered only datasets including more than 10 healthy subjects. As to June 30th 2020, only Illumina Infinium HumanMethylation450 datasets were retrieved. As described in the Results section, we applied additional selection criteria according to the different analysis, leaving the datasetsreported in Table 1 and Table 2.

Pre-processing

As raw intensities files were not available for some datasets, all the analyses were performed on pre-processed methylation data downloaded from GEO. Probes mapping on sex chromosomes and potentially ambiguous probes (cross-reactive probes and probes including SNPs) (47)were excluded, leaving 415016 probes. In each dataset, neuron/glia proportions were estimated using Horvath’s calculator(48).

Meta-anaysis

To identify differentially methylated positions (DMPs), the*lmFit* function implemented in *limma* R package (49)was used to fit a linear model to each microarray probe, expressing DNAm as Mvalues. Association with age was calculated using age as a continuous value and correcting for sex and neuron/glia proportion. Association with sex was calculated using sex as a categorical value and correcting for age and neuron/glia proportion. Association with AD was calculated using AD as a categorical value and correcting for age, sex and neuron/glia proportion. The *lmFit* function was used also to calculated the interaction between sex and age, correcting for neuron/glia proportion, and between AD and sex, correcting for age and neuron/glia proportion. Effect sizes and standard errors were extracted from *limma* output.For each brain region, the results obtained in the different datasets were combined by inverse variance-weighted fixed-effects meta-analysis using METAL

software (50). Finally, the p-values resulting from each meta-analysis were adjusted for multiple comparisons using the Benjamini-Hochberg (BH) procedure. Only probes with a BH-corrected p-value <0.01 and with concordant effect sizes between all the datasets included in each meta-analysis were retained as significant.

Enrichment and gene ontology analysis

Enrichment of genomic regions (Islands, N- and S-shores and shelves, open sea regions) was calculated using Fisher exact test, as implemented in the *fisher.test* function implemented in the stats R package. Enrichment of Gene Ontology terms was calculated using the *methylgometh* function implemented in the *methylGSA* R package (51), and redundant GO terms were removed by REViGO software (52).

RESULTS

DNA methylation datasets of healthy and AD human brains

We searched GEO database for datasets generated using the Illumina Infinium BeadChips on brain tissues from healthy and AD subjects (Materials and methods).

For the meta-analysis of sex- and age-dependent DNA methylation in healthy subjects, we selected only datasets including at least 10 males and 10 females, having a minimum of 20 years and spanning an age range of at least 30 years. We further considered only brain regions for which at least 2 datasets were available. This resulted in 8 datasets covering 4 regions: Frontal cortex (FC), Temporal cortex (TC), Entorhinal cortex (ERC), Cerebellum (CRB) (**Table 1**).

For the meta-analysis of AD-associated methylation patterns, we selected only the datasets including subjects over 65 years of age with at least 3 males and 3 females in the control and AD groups. This resulted in 8 datasets covering the same brain regions indicating above (**Table 2**).

DNA methylation differences across sex

To identify sex-dependent differentially methylated positions (sDMPs) we performed an epigenome wide association study (EWAS) in each dataset and brain region separately, correcting for age and estimated neuron/glia proportion (Materials and Methods). We then conducted a meta-analysis within each brain region.

We identified 4860 sDMPs in FC, 1985 sDMPs in TC, 159 sDMPs in ERC and 2322 sDMPs in CRB (**Figure 1A-D, Supplementary Figure 1and Supplementary File 1**). In FC, sDMPs were mainlyhypermethylated in males compared to females (73% of hypermethylated probes) while the opposite was true for TC,ERC and CRB (38%,33% and 36% of hypermethylated probes in TC,ERC and CRB respectively).When analyzing the genomic context of the sDMPs, we found that CpG islands were enriched in sDMPs in all the 4 brain regions, and that CpG island shores showed a similar trend (**Supplementary File 2**).Also the distribution of sDMPs across chromosomes was not random, with a trend towards enrichment in chromosome 19 in all the 4 brain regions.The enrichment analysis of Gene Ontology (GO) terms did not reveal significant results except for FC, where the “homophilic cell adhesion via plasma membrane adhesion molecules” ontologywas found (**SupplementaryFile 2**).

To investigate whether sex-dependent DNA methylation changes were consistent across brain regions, we evaluated the correlation of effect size values between FC, TC, ERC and CRB (Figure

2A). The 4 brain regions were positively correlated each other (**Figure 2A)**.We next intersected the 4sDMPs lists,identifying77 common probes mapping in 57genes (**Figure 2D, Table 3** and **Supplementary File 1**). All these probes showed concordant sex-dependent DNA methylation profiles in the 4 brain regions and most of them (73%) were hypomethylated in males.
On the other hand, we searched for probes having sex-related DNAm differences only in one brain region(region-specific sDMPs; Materials and Methods). We found 2, 4, 0 and 37region-specific sDMPs in FC, TC, ERC and CRB respectively (**Supplementary File 1**). Interestingly, 5sDMPs specific for CRB mapped all in the same gene, Nuclear Enriched Abundant Transcript 1 (NEAT1) (**Figure 3**).

DNA methylation changes across age

To identify age-dependent differentially methylated positions (aDMPs) we performed an EWAS in each dataset and brain region separately, correcting for sex and estimated neuron/glia proportion (Materials and Methods). We then conducted a meta-analysis within each brain region.
We identified 24581, 10077, 404 and 1140 aDMPs in FC, TC, ERC and CRB respectively (**Figures1E-H, Supplementary Figure 2E** and **Supplementary File 3**). In all brain regions, most of theaDMPsunderwent hypermethylation with age (76%, 88%, 58% and 62% of hypermethylatedaDMPs in FC, RC, ERC and CRB respectively). The genomic context of aDMPs was not consistent across the 4 brain regions, except for a significant under-representationin “open sea” regions (**Supplementary File 4**). Similarly, aDMPs were differently scattered across chromosomes in FC, TC, ERC and CRB. GO enrichment analysis revealed several pathways involved in morphogenesis anddevelopmentalprocesses, with “pattern specification process” and “regionalization” common to FC, TC and ERC (**Supplementary File 4**).
The analysis of correlation between the effect sizes revealed that age-associated changes were more similar between FC and TC compared to the other regions (**Figure 2B)**.The intersection of the aDMPs from the 4 brain regions highlighted 28 common probes, all concordantly undergoing hypermethylation with age and mapping in 25 genes (**Figure 2E and Table 4**). The opposite analysis, *i.e.* the identification of region-specific aDMPs (Materials and Methods), identified only 1 probe specific for FC (cg01725130), that maps in the body of Ras And Rab Interactor 3 (RIN3) gene (**Supplementary File 2**).

Relation between age and sex in brain DNA methylation

We then aimed at studying how sex-specific brain DNAm is modulated during aging.
First of all, we intersected sDMPs and aDMPslists. In FC, we found 675 probes that change with sex and with age (s&aDMPs), corresponding to about 13% of all sDMPs identified. In TC s&aDMPs were 171, corresponding to 8.5%of sDMPs. In ERC we found only 2s&aDMPs, while in CRBs&aDMPswere 19, corresponding to 4% of sDMPs(**Figure 4 and Supplementary Files 1 and 3**). In all the four regions, the proportion of sDMPs changing with age (i.e., the proportion of s&aDMPs) was higher than expected (Fisher’s Exact Test p-value <0.05; odds ratio of 2.6, 3.8,13.0 and3.0 in FC, TC, ERC and CRB respectively). InFC, TC and CRB, most of the s&aDMPs were probes having higher DNAm levels in males respect to females and undergoing hypermethylation during aging. GO analysis revealed only 1 ontology enriched in FC (“homophilic cell adhesion via plasma membrane adhesion molecules”).
The previous analysis identifies CpG probes whose DNAm changes according to both sex and age, but is not informative about possible differences in aging trajectories between males and females.

To fulfill this point, we performed an age-by-sex interaction analysis in each dataset(Materials and Methods) and meta-analyzed the results for the 4 brain regions. Only 4, 4, 2 and 2 probes showed a significant age-by-sex interaction in FC, TC, ERC and CRB respectively (**Supplementary File 5**).

Brain DNA methylation changes across AD

Finally, we focused on brain DNAm datasets including late onset AD patients (LOAD) and age-matched non-demented controls.

To identify differentially methylated positions associated with LOAD (LOAD-DMPs) we performed an EWAS in each dataset and brain region separately, correcting for age, sex and estimated neuron/glia proportion (materials and methods). We then conducted a meta-analysis within each brain region.

We identified14 LOAD-DMPs in FC, 5405 in TC, 47 in ERC and only 1 in CRB (**Figures 1I-N**), **Supplementary Figure 3** and **Supplementary File 6**). In all brain regions most of LOAD-DMPs were hypermethylated in AD compared to controls (93%,80%, 76% and 100% in FC, TC, ERC and CRB respectively).While in TC LOAD-DMPs were significantly under-represented in CpG islands and enriched in the other genomic contexts, a significant enrichment in CpG islands was found for LOAD-DMPs identified in FC (**Supplementary File 7**). GO analysis returned significant results only in TC, where pathways related to synapse organization and function were found (**Supplementary File 7**).

Correlation analysis of effect size between 4 brain regions highlighted a distinctive pattern in CRB respect to FC, TC and ERC, while the correlation was higher between TC and ERC (**Figure 2C**). Accordingly the intersection between LOAD-DMPs in the 4 brain regions did not return common probes, while 29 probes (mapping in 23 genes)and 8 probes (mapping in 6 genes) were identified by intersecting TC and ERCor FC and TC, respectively (**Figure 2F**and **Table 5**). The probecg12163800, mapping in Rhomboid 5 Homolog 2 (RHBDF2) gene, was significantly hypermethylated in FC, TC and ERC from AD patients.

Relation between sex- and age-associatedDNAm changes and AD epigenetic remodeling

Finally, we explored whether AD-associated DNAm changes were related to sex- and age-specific brain DNAm patterns occurring in physiological conditions, identified in the above described analyses.

In each brain region, we intersected the LOAD-DMPs and sDMPs in orderto identify LOAD&sDMPs, *i.e.* probes that have basal differential DNAm between the two sexes and are also affected by AD.The intersection did not result in any probe for all the regions except that for TC, where we found 23LOAD&sDMPs, mapping in 16 genes and corresponding to only0.4% of LOAD-DMPs in TC (Fisher's Exact Test p-value >0.05)(**Figure 4**and**Supplementary Files 1 and 6)**.Moreover, AD-by-sex interaction analysis yielded no significant probes in any regions.

Similarly, we explored whether LOAD-DMPs occur in probes whose DNAm changes during physiological aging process (LOAD&aDMPs). The intersection between LOAD-DMPs and aDMPs highlighted 7, 456, 4 and 0 probes in FC, TC, ERC and CRB respectively(**Figure 4**).The proportion of LOAD&aDMPs was higher than expected by chance in FC, TC and ERC (Fisher's Exact Test p-value <0.05; odds ratio of 15.9, 3.8 and 95in FC, TC and ERC respectively). We found that the 87% of LOAD&aDMPs in TC are concordant for the effect size sign between aDMPs and LOAD-DMPs, while this percentage reached 100% in FC e ERC. Notably, the 4LOAD&aDMPsfound in ERC (cg11823178, cg03169557, cg25018458 and cg22090150, mapping in SPG7 Matrix AAA

Peptidase Subunit, Paraplegin [SPG7], Ankyrin1 [ANK1/MIR486], Ankyrin Repeat And FYVE Domain Containing 1 [ANKFY1] and ABR Activator Of RhoGEF And GTPase [ABR] respectively)were also found in TC.Also the intersection between LOAD&aDMPs in TC and FC resulted in 4 common probes: cg22962123, mapping in PDZ And LIM Domain 2 (PDLIM2) gene; cg07061298, not mapping in any gene; cg01463828 and cg04874795, both mapping in Homeobox A3 (HOXA3) gene. Figure 5 reports DNAm values of cg11823178 (ANK1) and cg22962123 (PDLIM2) in TC from GSE134379 dataset as an example of CpG sites displaying a positive association of DNAm with age and hypermethylated in AD.
Finally, it is worth to note that TC is the exclusive brain region in which we found probes at the intersection between aDMPs, sDMPs and LOAD-DMPs (LOAD&a&sDMPs)(**Figure 4B**).The 5 probes (cg20225999, cg03951603, cg08820801, cg22263793, cg10828284) which mapped inF-Box Protein 17 (FBXO17), Mov10 Like RISC Complex RNA Helicase 1(MOV10L1)genes were all hypermethylated in males and with aging; three of them (cg20225999, cg08820801, cg10828284) were further hypermethylated in AD.

DISCUSSION

Sex and age are among the major risk factors for AD. In this paper we performed a meta-analysis of DNAm changes that are associated to sex and aging in 4 brain regions (FC, TC, ERC, CRB) and we evaluated whether they contribute to the epigenetic alterations that have been widely described in AD. Our main findings are summarized in the following paragraphs.

Sex-dependent DNAm differences tend to be shared between brain regions, with few exceptions

To date some studies have reported DNAm sex differences in human brain, mainly focusing on frontal cortex (29-31, 42) with few exceptions (28). Our meta-analysis confirms the presence of autosomic probes with differential methylation between males and females in all the brain regions. These probes preferentially map in CpG islands and shores suggesting their involvement in the regulation of sex-specific gene expression in brain(31).
Sex specific DNAm tend to be reproducible across the brain regions and 77 CpGs resulted from the cross-region intersection. Among them there are sDMPs mapping in genes that have been already associated to sex differences in brain physiology and pathology, likePar-3 Family Cell Polarity Regulator Beta (PARD3B)(53), DEAF1 Transcription Factor (DEAF1)(54) and Iodothyronine Deiodinase 3 (DIO3)(55) genes. Most of these 77 probes were previously reported as differentially methylated between males and females also in previous meta-analysis on blood(56, 57).
In addition, we found few examples of sDMPs specific for a brain region. The most notable example is in cerebellum and maps in NEAT1. NEAT1 is a ubiquitously expressed long non-coding RNA (lncRNA) involved in a plethora of neurospecific processes such as brain development and aging (58-60). Recent transcriptomic studies on human CNS revealed altered NEAT1 levels in AD (61),PD (62) and in schizophrenia (63).

DNAm tends to be differently remodeled during aging according to the brain region

Several studies have analyzed age-associated changes in DNAm in brain, both comparing fetal *versus* adult brains and analyzing methylation profiles across adulthood(13, 16, 38, 64-67). Our meta-analysis showes that during aging there is an increase of methylation at specific loci,

accordingly to previously published data on blood (56, 68)and brain (38). As previously reported by Hernandez et al (38), also our results support the involvement of brain aDMPs in GO related to developmental processes and morphogenesis. Furthermore, our meta-analysis confirms and extends the observation that the epigenome is differently remodeled during aging across brain regions(38).In particular we observed thatage-associated DNAm patterns are similar in TC and FC, while they are distinct in ERC and CRB. CRB was previously described to undergo to a peculiar epigenetic aging, which was decelerated according to Horvath's epigenetic clock(37).
The large fraction (93%) of the 28 aDMPs emerged from our cross region analysis was found also in aging studies on blood (56). Among them there are probes mapping in Four And A Half LIM Domains 2 (FHL2) and ELOVL Fatty Acid Elongase 2 (ELOVL2) genes, previously reported as age-associated in large number of studies on several tissues (69, 70)including sorted neuron and glia cells(16). According to what discussed above and to previous results (69, 71) the effect size of ELOVL2 probe cg16867657 was lower in CRB respect the other regions, but still significant in our meta-analysis. Elovl2 is an enzyme involved in the elongation of fatty acids and its functional role in aging has been recently suggested (72).

Sites with sex-dependent DNAm are similarly modulated during aging in males and females
Previous studies in mice and humans suggested that, while sex-differences in DNAm at certain CpG sites are maintained during life, other CpG sites show sexually divergent aging patterns, *i.e* they have a different response to aging in males and females(42). Our meta-analysis supports the fact that sDMPs have a high propensity to be modulated during aging, as the intersection of sDMPs and aDMPs is higher than expected in all the 4 brain regions. However, we found only few probes with significant sex-by-age interaction, indicating similar rather than diverging changes in DNAm in males and females aging. The discrepancy between our results and previous findingscan be due to different reasons: for example, while Masser et al. considered only one dataset including frontal cortex data, here we meta-analysed several datasets using selective criteria of concordance between all datasets from the same brain region; furthermore, we applied a filtering step that removed potentially ambiguous probes, thus reducing the potential overlap with Masser's results. Our results are more similar to what reported by two independent studies in blood (41, 56),which showed that only a small fraction of CpGs have significant sex-by-age interaction. Further studies on larger cohorts are needed to better describe sex-dependent DNAm patterns during brain aging.

Epigenetic changes in AD are enriched in sites that show age- but not sex-dependent DNAm
A recent meta-analysis on EWAS studies identified 220 CpGs associated with AD neuropathology, shared by brain cortical cortex regions but not by CRB(73). The paper by Smith et al. included several datasets that we used also in our meta-analysis, with the exception of GSE125895 and GSE109627, while we did not have access to the ROS/MAP and RBD DNAm data. Furthermore, while Smith et al. considered the association with Braak stage, here we used the disease as a binary trait (affected/unaffected). Despite these differences, our results largely overlap with those previously reported. In particular, we did not find AD-related probes common to all the 4 brain regions that we investigated, with CRB DNAm clearly less affected by the pathology. On the contrary, a subset of sites was shared between FC, TC and ERC, and about 50% of these probes overlap with published data. These probes map within genes whose epigenetic deregulation has been largely documented in AD, including *ANK1*, *RHBDF2* and *HOXA3*. On the contrary, we did

not find any overlapwhen comparing our results on AD brain with CpG sites identified in AD patients' blood (74), confirming that the pathology differently affects the two tissues as recently reported(75).

We did not find a significant overlap between LOAD-DMPs and sDMPs, nor we found significant interaction effects between sex and AD. Overall these results suggest that AD does not predominantly insist on sites with sex-specific DNAm, and that the epigenetic differences between the two sexes do not contribute to the different prevalence of the disease in males and females.

Conversely, our data show that in FC, TC and ERC, AD-related epigenetic modifications are significantly enriched in probes whose DNAm changes with age. Strikingly, we found a high concordance between the direction of DNAm changes (hyper or hypo-methylation)in LOAD&aDMPs, indicating that a subset of age-associated DNAm changes are exaggerated in AD. In TC, LOAD&aDMPs included probes mapping in*ANK1*, and it is worth to note that the down-regulation of Ank2 (ANK1 human orthologue gene) in *Drosophila* has been associated to memory loss, neuronal dysfunction and shortened lifespan in a recent report(76).

Overall, these results support a geroscience view(77-80)according to which AD can be considered a deviation of the physiological aging trajectories towards accelerated aging. Epigenetic age acceleration was previously reported in AD neurons, were a pronounced loss of CpH methylation was found at enhancers, similar to what observed in aging, and in bulk prefrontal cortex, where epigenetic age calculated by Horvath's clock was positively associated with neuritic plaques and amyloid load (81). It will be interesting to know whether similar results will be obtained using the recently published epigenetic clock optimized for brain tissues(82).

Strengths, limitations and conclusion

To the best of our knowledge, this is the first report in which sex-, age- and AD-related DNAm changes are systematically assessed using the same analytical approach. Furthermore, we used stringent selection criteria that enabled to select only probes with concordant DNAm changes in the different datasets. On the other side, our study has some limitations. The datasets that we meta-analysed largely vary in size and age range of the assessed subjects, an aspect important for the identification of aDMPs. Moreover, in all the datasets it was not possible to distinguish 5-methylcytosine from 5-hydroxymethylcytosine, an epigenetic modification that contributes to both brain function and neurodegeneration(17, 73, 83, 84). Finally, the datasets that we meta-analysed were based on bulk brain tissues. Although all the analyses were corrected for neuron/glia proportions predicted from DNAm data, we cannot exclude that the observed sex-, age- and LOAD-associated DNAm changes are at least in part driven by changes in brain cells composition that occur in physiological and pathological conditions. For example, Gasparoni et al reported that ANK1 deregulation in AD is specific for glial cells (16), a finding further supported by gene expression studies (85), and that the epigenetic profiles of neurons and glia are differently modulated during aging. Notwithstanding, our results suggest that (cell-specific) age-associated remodelling of DNAm is not just a confounding factor for the epigenetic deregulation observed in AD, but on the contrary it is the predisposing *milieu* in which AD pathogenetic mechanisms are established.

In conclusion, we demonstrated that age-associated, but not sex-associated DNAm patterns concurs to the epigenetic deregulation observed in AD, providing new insight on how advanced age enables neurodegeneration.

Abbreviations

DNAm: DNA methylation
AD: Alzheimer's Disease
DMPs:differentially methylated positions
LOAD: Late Onset Alzheimer's Disease
EWAS: Epigenome-Wide Association Study
GO: Gene Ontology
sDMPs: sex-associated differentially methylated positions
aDMPs: age-associated differentially methylated positions
s&aDMPs: sex- and age-associated differentially methylated positions
LOAD&aDMPs: Late Onset Alzheimer's Disease-specific age-associated differentially methylated positions
LOAD&sDMPs: Late Onset Alzheimer's Disease-specific sex-associated variably methylated positions
LOAD&a&sDMPs: Late Onset Alzheimer's Disease-specific sex- and age-associated variably methylated positions

Conflicts of Interest

The authors declare that they have no competing interests.

REFERENCES

1. Coupé P, Manjón JV, Lanuza E, Catheline G. Lifespan Changes of the Human Brain In Alzheimer's Disease. Scientific Reports. 2019;9(1):3998.
2. Van Hoesen GW, Hyman BT, Damasio AR. Entorhinal cortex pathology in Alzheimer's disease. Hippocampus. 1991;1(1):1-8.
3. Braak H, Braak E. Neuropathological stageing of Alzheimer-related changes. Acta Neuropathol. 1991;82(4):239-59.
4. Scahill RI, Schott JM, Stevens JM, Rossor MN, Fox NC. Mapping the evolution of regional atrophy in Alzheimer's disease: unbiased analysis of fluid-registered serial MRI. Proceedings of the National Academy of Sciences of the United States of America. 2002;99(7):4703-7.
5. Fisher DW, Bennett DA, Dong H. Sexual dimorphism in predisposition to Alzheimer's disease. Neurobiol Aging. 2018;70:308-24.
6. Podcasy JL, Epperson CN. Considering sex and gender in Alzheimer disease and other dementias. Dialogues in clinical neuroscience. 2016;18(4):437-46.
7. Hickman RA, Faustin A, Wisniewski T. Alzheimer Disease and Its Growing Epidemic: Risk Factors, Biomarkers, and the Urgent Need for Therapeutics. Neurologic clinics. 2016;34(4):941-53.
8. Kawas CH, Corrada MM. Alzheimer's and dementia in the oldest-old: a century of challenges. Current Alzheimer research. 2006;3(5):411-9.
9. Hebert LE, Scherr PA, Beckett LA, Albert MS, Pilgrim DM, Chown MJ, et al. Age-Specific Incidence of Alzheimer's Disease in a Community Population. JAMA. 1995;273(17):1354-9.
10. Nebel RA, Aggarwal NT, Barnes LL, Gallagher A, Goldstein JM, Kantarci K, et al. Understanding the impact of sex and gender in Alzheimer's disease: A call to action. Alzheimers Dement. 2018;14(9):1171-83.
11. Pike CJ. Sex and the development of Alzheimer's disease. Journal of neuroscience research. 2017;95(1-2):671-80.
12. Fagiolini M, Jensen CL, Champagne FA. Epigenetic influences on brain development and plasticity. Curr Opin Neurobiol. 2009;19(2):207-12.

13. Jaffe AE, Gao Y, Deep-Soboslay A, Tao R, Hyde TM, Weinberger DR, et al. Mapping DNA methylation across development, genotype and schizophrenia in the human frontal cortex. Nat Neurosci. 2016;19(1):40-7.
14. Landgrave-Gómez J, Mercado-Gómez O, Guevara-Guzmán R. Epigenetic mechanisms in neurological and neurodegenerative diseases. Front Cell Neurosci. 2015;9:58.
15. Altuna M, Urdánoz-Casado A, Sánchez-Ruiz de Gordoa J, Zelaya MV, Labarga A, Lepesant JMJ, et al. DNA methylation signature of human hippocampus in Alzheimer's disease is linked to neurogenesis. Clin Epigenetics. 2019;11(1):91.
16. Gasparoni G, Bultmann S, Lutsik P, Kraus TFJ, Sordon S, Vlcek J, et al. DNA methylation analysis on purified neurons and glia dissects age and Alzheimer's disease-specific changes in the human cortex. Epigenetics Chromatin. 2018;11(1):41.
17. Lardenoije R, Roubroeks JAY, Pishva E, Leber M, Wagner H, Iatrou A, et al. Alzheimer's disease-associated (hydroxy)methylomic changes in the brain and blood. Clin Epigenetics. 2019;11(1):164.
18. Semick SA, Bharadwaj RA, Collado-Torres L, Tao R, Shin JH, Deep-Soboslay A, et al. Integrated DNA methylation and gene expression profiling across multiple brain regions implicate novel genes in Alzheimer's disease. Acta Neuropathol. 2019;137(4):557-69.
19. Smith AR, Smith RG, Pishva E, Hannon E, Roubroeks JAY, Burrage J, et al. Parallel profiling of DNA methylation and hydroxymethylation highlights neuropathology-associated epigenetic variation in Alzheimer's disease. Clin Epigenetics. 2019;11(1):52.
20. Smith AR, Wheildon G, Lunnon K. A five-year update on epigenome-wide association studies of DNA modifications in Alzheimer's disease: progress, practicalities and promise. Neuropathol Appl Neurobiol. 2020.
21. Wei X, Zhang L, Zeng Y. DNA methylation in Alzheimer's disease: in brain and peripheral blood. Mech Ageing Dev. 2020:111319.
22. Lunnon K, Smith R, Hannon E, De Jager PL, Srivastava G, Volta M, et al. Methylomic profiling implicates cortical deregulation of ANK1 in Alzheimer's disease. Nature neuroscience. 2014;17(9):1164-70.
23. Smith RG, Hannon E, De Jager PL, Chibnik L, Lott SJ, Condliffe D, et al. Elevated DNA methylation across a 48-kb region spanning the HOXA gene cluster is associated with Alzheimer's disease neuropathology. Alzheimers Dement. 2018;14(12):1580-8.
24. Smith RG, Pishva E, Shireby G, Smith AR, Roubroeks JAY, Hannon E, et al. Meta-analysis of epigenome-wide association studies in Alzheimer’s disease highlights novel differentially methylated loci across cortex. bioRxiv. 2020:2020.02.28.957894.
25. Gilbert TM, Zürcher NR, Catanese MC, Tseng CJ, Di Biase MA, Lyall AE, et al. Neuroepigenetic signatures of age and sex in the living human brain. Nat Commun. 2019;10(1):2945.
26. Singmann P, Shem-Tov D, Wahl S, Grallert H, Fiorito G, Shin S-Y, et al. Characterization of whole-genome autosomal differences of DNA methylation between men and women. Epigenetics & Chromatin. 2015;8(1):43.
27. Maschietto M, Bastos LC, Tahira AC, Bastos EP, Euclydes VL, Brentani A, et al. Sex differences in DNA methylation of the cord blood are related to sex-bias psychiatric diseases. Sci Rep. 2017;7:44547.
28. Xia Y, Dai R, Wang K, Jiao C, Zhang C, Xu Y, et al. Sex-differential DNA methylation and associated regulation networks in human brain implicated in the sex-biased risks of psychiatric disorders. Mol Psychiatry. 2019.
29. Spiers H, Hannon E, Schalkwyk LC, Smith R, Wong CC, O'Donovan MC, et al. Methylomic trajectories across human fetal brain development. Genome Res. 2015;25(3):338-52.
30. Perzel Mandell KA, Price AJ, Wilton R, Collado-Torres L, Tao R, Eagles NJ, et al. Characterizing the dynamic and functional DNA methylation landscape in the developing human cortex. Epigenetics. 2020:1-13.

31. Xu H, Wang F, Liu Y, Yu Y, Gelernter J, Zhang H. Sex-biased methylome and transcriptome in human prefrontal cortex. Hum Mol Genet. 2014;23(5):1260-70.
32. McCarthy MM, Auger AP, Bale TL, De Vries GJ, Dunn GA, Forger NG, et al. The epigenetics of sex differences in the brain. J Neurosci. 2009;29(41):12815-23.
33. Forger NG. Epigenetic mechanisms in sexual differentiation of the brain and behaviour. Philos Trans R Soc Lond B Biol Sci. 2016;371(1688):20150114.
34. Gegenhuber B, Tollkuhn J. Sex Differences in the Epigenome: A Cause or Consequence of Sexual Differentiation of the Brain? Genes (Basel). 2019;10(6).
35. Pal S, Tyler JK. Epigenetics and aging. Science advances. 2016;2(7):e1600584-e.
36. Xiao F-H, Wang H-T, Kong Q-P. Dynamic DNA Methylation During Aging: A "Prophet" of Age-Related Outcomes. Frontiers in Genetics. 2019;10:107.
37. Horvath S, Mah V, Lu AT, Woo JS, Choi OW, Jasinska AJ, et al. The cerebellum ages slowly according to the epigenetic clock. Aging (Albany NY). 2015;7(5):294-306.
38. Hernandez DG, Nalls MA, Gibbs JR, Arepalli S, van der Brug M, Chong S, et al. Distinct DNA methylation changes highly correlated with chronological age in the human brain. Hum Mol Genet. 2011;20(6):1164-72.
39. Bishop NA, Lu T, Yankner BA. Neural mechanisms of ageing and cognitive decline. Nature. 2010;464(7288):529-35.
40. Lardenoije R, Iatrou A, Kenis G, Kompotis K, Steinbusch HWM, Mastroeni D, et al. The epigenetics of aging and neurodegeneration. Progress in neurobiology. 2015;131:21-64.
41. McCartney DL, Zhang F, Hillary RF, Zhang Q, Stevenson AJ, Walker RM, et al. An epigenome-wide association study of sex-specific chronological ageing. Genome Med. 2019;12(1):1.
42. Masser DR, Hadad N, Porter HL, Mangold CA, Unnikrishnan A, Ford MM, et al. Sexually divergent DNA methylation patterns with hippocampal aging. Aging Cell. 2017;16(6):1342-52.
43. Horvath S, Gurven M, Levine ME, Trumble BC, Kaplan H, Allayee H, et al. An epigenetic clock analysis of race/ethnicity, sex, and coronary heart disease. Genome Biol. 2016;17(1):171.
44. Xiao FH, Chen XQ, He YH, Kong QP. Accelerated DNA methylation changes in middle-aged men define sexual dimorphism in human lifespans. Clin Epigenetics. 2018;10(1):133.
45. Tajuddin SM, Hernandez DG, Chen BH, Noren Hooten N, Mode NA, Nalls MA, et al. Novel age-associated DNA methylation changes and epigenetic age acceleration in middle-aged African Americans and whites. Clin Epigenetics. 2019;11(1):119.
46. Clough E, Barrett T. The Gene Expression Omnibus Database. Methods Mol Biol. 2016;1418:93-110.
47. Zhou W, Laird PW, Shen H. Comprehensive characterization, annotation and innovative use of Infinium DNA methylation BeadChip probes. Nucleic Acids Res. 2017;45(4):e22.
48. Horvath S. DNA methylation age of human tissues and cell types. Genome Biol. 2013;14(10):R115.
49. Ritchie ME, Phipson B, Wu D, Hu Y, Law CW, Shi W, et al. limma powers differential expression analyses for RNA-sequencing and microarray studies. Nucleic Acids Res. 2015;43(7):e47.
50. Willer CJ, Li Y, Abecasis GR. METAL: fast and efficient meta-analysis of genomewide association scans. Bioinformatics. 2010;26(17):2190-1.
51. Ren X, Kuan PF. methylGSA: a Bioconductor package and Shiny app for DNA methylation data length bias adjustment in gene set testing. Bioinformatics. 2019;35(11):1958-9.
52. Supek F, Bošnjak M, Škunca N, Šmuc T. REVIGO Summarizes and Visualizes Long Lists of Gene Ontology Terms. PLOS ONE. 2011;6(7):e21800.
53. Phillips OR, Onopa AK, Hsu V, Ollila HM, Hillary RP, Hallmayer J, et al. Beyond a Binary Classification of Sex: An Examination of Brain Sex Differentiation, Psychopathology, and Genotype. J Am Acad Child Adolesc Psychiatry. 2019;58(8):787-98.

54. Luckhart C, Philippe TJ, Le François B, Vahid-Ansari F, Geddes SD, Béïque JC, et al. Sex-dependent adaptive changes in serotonin-1A autoreceptor function and anxiety in Deaf1-deficient mice. Mol Brain. 2016;9(1):77.
55. Stohn JP, Martinez ME, St Germain DL, Hernandez A. Adult onset of type 3 deiodinase deficiency in mice alters brain gene expression and increases locomotor activity. Psychoneuroendocrinology. 2019;110:104439.
56. Yusipov I, Bacalini MG, Kalyakulina A, Krivonosov M, Pirazzini C, Gensous N, et al. Age-related DNA methylation changes are sex-specific: a comprehensive assessment. bioRxiv. 2020:2020.01.15.905224.
57. McCarthy NS, Melton PE, Cadby G, Yazar S, Franchina M, Moses EK, et al. Meta-analysis of human methylation data for evidence of sex-specific autosomal patterns. BMC Genomics. 2014;15(1):981.
58. An H, Williams NG, Shelkovnikova TA. NEAT1 and paraspeckles in neurodegenerative diseases: A missing lnc found? Non-coding RNA research. 2018;3(4):243-52.
59. Pereira Fernandes D, Bitar M, Jacobs FMJ, Barry G. Long Non-Coding RNAs in Neuronal Aging. Non-coding RNA. 2018;4(2):12.
60. Salvatori B, Biscarini S, Morlando M. Non-coding RNAs in Nervous System Development and Disease. Frontiers in cell and developmental biology. 2020;8:273-.
61. Spreafico M, Grillo B, Rusconi F, Battaglioli E, Venturin M. Multiple Layers of. Int J Mol Sci. 2018;19(7).
62. Simchovitz A, Hanan M, Niederhoffer N, Madrer N, Yayon N, Bennett ER, et al. NEAT1 is overexpressed in Parkinson's disease substantia nigra and confers drug-inducible neuroprotection from oxidative stress. FASEB J. 2019;33(10):11223-34.
63. Katsel P, Roussos P, Fam P, Khan S, Tan W, Hirose T, et al. The expression of long noncoding RNA NEAT1 is reduced in schizophrenia and modulates oligodendrocytes transcription. NPJ Schizophr. 2019;5(1):3.
64. Horvath S, Zhang Y, Langfelder P, Kahn RS, Boks MP, van Eijk K, et al. Aging effects on DNA methylation modules in human brain and blood tissue. Genome Biol. 2012;13(10):R97.
65. Day K, Waite LL, Thalacker-Mercer A, West A, Bamman MM, Brooks JD, et al. Differential DNA methylation with age displays both common and dynamic features across human tissues that are influenced by CpG landscape. Genome Biol. 2013;14(9):R102.
66. Price AJ, Collado-Torres L, Ivanov NA, Xia W, Burke EE, Shin JH, et al. Divergent neuronal DNA methylation patterns across human cortical development reveal critical periods and a unique role of CpH methylation. Genome Biology. 2019;20(1):196.
67. Numata S, Ye T, Hyde TM, Guitart-Navarro X, Tao R, Wininger M, et al. DNA methylation signatures in development and aging of the human prefrontal cortex. Am J Hum Genet. 2012;90(2):260-72.
68. Xiao F-H, Kong Q-P, Perry B, He Y-H. Progress on the role of DNA methylation in aging and longevity. Briefings in Functional Genomics. 2016;15(6):454-9.
69. Slieker RC, Relton CL, Gaunt TR, Slagboom PE, Heijmans BT. Age-related DNA methylation changes are tissue-specific with ELOVL2 promoter methylation as exception. Epigenetics & Chromatin. 2018;11(1):25.
70. Garagnani P, Bacalini MG, Pirazzini C, Gori D, Giuliani C, Mari D, et al. Methylation of ELOVL2 gene as a new epigenetic marker of age. Aging Cell. 2012;11(6):1132-4.
71. Bacalini MG, Deelen J, Pirazzini C, De Cecco M, Giuliani C, Lanzarini C, et al. Systemic Age-Associated DNA Hypermethylation of ELOVL2 Gene: In Vivo and In Vitro Evidences of a Cell Replication Process. The journals of gerontology Series A, Biological sciences and medical sciences. 2017;72(8):1015-23.
72. Chao DL, Skowronska-Krawczyk D. ELOVL2: Not just a biomarker of aging. Transl Med Aging. 2020;4:78-80.

73. Smith AR, Smith RG, Pishva E, Hannon E, Roubroeks JAY, Burrage J, et al. Parallel profiling of DNA methylation and hydroxymethylation highlights neuropathology-associated epigenetic variation in Alzheimer's disease. Clinical Epigenetics. 2019;11(1):52.
74. Roubroeks JAY, Smith AR, Smith RG, Pishva E, Ibrahim Z, Sattlecker M, et al. An epigenome-wide association study of Alzheimer's disease blood highlights robust DNA hypermethylation in the HOXB6 gene. Neurobiol Aging. 2020;95:26-45.
75. Wei X, Zhang L, Zeng Y. DNA methylation in Alzheimer's disease: In brain and peripheral blood. Mechanisms of Ageing and Development. 2020;191:111319.
76. Higham JP, Malik BR, Buhl E, Dawson JM, Ogier AS, Lunnon K, et al. Alzheimer's Disease Associated Genes Ankyrin and Tau Cause Shortened Lifespan and Memory Loss in Drosophila. Frontiers in Cellular Neuroscience. 2019;13:260.
77. Sierra F. Editorial: Geroscience and the Role of Aging in the Etiology and Management of Alzheimer's Disease. J Prev Alzheimers Dis. 2020;7(1):2-3.
78. Kennedy BK, Berger SL, Brunet A, Campisi J, Cuervo AM, Epel ES, et al. Geroscience: linking aging to chronic disease. Cell. 2014;159(4):709-13.
79. Trevisan K, Cristina-Pereira R, Silva-Amaral D, Aversi-Ferreira TA. Theories of Aging and the Prevalence of Alzheimer's Disease. Biomed Res Int. 2019;2019:9171424.
80. Xia X, Jiang Q, McDermott J, Han JJ. Aging and Alzheimer's disease: Comparison and associations from molecular to system level. Aging Cell. 2018;17(5):e12802.
81. Levine ME, Lu AT, Bennett DA, Horvath S. Epigenetic age of the pre-frontal cortex is associated with neuritic plaques, amyloid load, and Alzheimer's disease related cognitive functioning. Aging (Albany NY). 2015;7(12):1198-211.
82. Shireby GL, Davies JP, Francis PT, Burrage J, Walker EM, Neilson GWA, et al. Recalibrating the epigenetic clock: implications for assessing biological age in the human cortex. Brain. 2020.
83. Coppieters N, Dieriks BV, Lill C, Faull RL, Curtis MA, Dragunow M. Global changes in DNA methylation and hydroxymethylation in Alzheimer's disease human brain. Neurobiol Aging. 2014;35(6):1334-44.
84. Ellison EM, Bradley-Whitman MA, Lovell MA. Single-Base Resolution Mapping of 5-Hydroxymethylcytosine Modifications in Hippocampus of Alzheimer's Disease Subjects. J Mol Neurosci. 2017;63(2):185-97.
85. Mastroeni D, Sekar S, Nolz J, Delvaux E, Lunnon K, Mill J, et al. ANK1 is up-regulated in laser captured microglia in Alzheimer's brain; the importance of addressing cellular heterogeneity. PLoS One. 2017;12(7):e0177814.

Figure legend

Figure 1. Sex-, age- and AD- associated epigenetic remodeling in the four brain regions. Volcano plots of -log10(P-value) against effect sizes, resulting from the meta-analysis of: sex-associated DMPs in FC **(A)**, TC **(B)**, ERC **(C)** and CRB **(D)**; age-associated DMPs in FC **(E)**, TC **(F)**, ERC **(G)** and CRB **(H)**; LOAD-associated DMPs in FC **(I)**, TC **(L)**, ERC **(M)** and CRB **(N)**. Significant probes (BH-corrected p-value < 0.05) are colored in black.

Figure 2. Cross-region analysis of sex-, age- and AD-associated probes. (A-C) Correlation matrix plots show the magnitude of correlation between probes effect sizes in the 4 brain regions, considering the result of the meta-analysis onsex- (**A**), age- (**B**) and AD- (**C**) associated probes. Positive and negative correlation values are indicatedin blue and red respectively. **(D-F)** Venn diagrams display the number of significant DMPs shared between the 4 brain regions, considering sDMPs (**D**), aDMPs (**E**) and LOAD-DMPs (**F**). The genes in which map the most shared probes are reported below each diagram.

Figure 3. CRB-specific sex-associated DNAm of NEAT1 gene. Forest plot of the three CRB-specific sDMPs mapping in*NEAT1*gene: (**A**) cg16884222, (**B**) cg09411730, (**C**) cg07985890. For each probe, effect sizes from the datasets used for our meta-analysis are reported, dividing them according to the 4 brain regions (CRB, yellow; FC, magenta; TC, cyan; ERC, gray)

Figure 4. Intersections of sex-, age- and AD-associated probes in each of the four brain regions. Venn diagrams depict the intersection between sDMPs, aDMPs and LOAD-DMPs in FC (**A**), TC (**B**), ERC (**C**) and CRB (**D**).

Figure 5. Scatter plots of *ANK1* and *PDLIM2* DNAm according to age and disease. Scatter plots of methylation values of cg11823178 within *ANK1*(**A**) and of cg22962123 within *PDLIM2* (**B**) in TC from GSE134379 dataset). Healthy subjects are colored in gray while AD patients are in orange. Regression lines and interval confidence within each group are reported.

Supplementary Figures

Supplementary Figure 1. Manhattan plots of sDMPs in the four brain regions. The figure displays the Manhattan plots resulting from the meta-analysis of sex-associated probes in FC (**A**), TC (**B**), ERC (**C**) and CRB (**D**). Significant sDMPs are marked with dark color. Scale change across 50 is indicated by an axis break.

Supplementary Figure 2. Manhattan plots of aDMPs in the four brain regions. The figure displays the Manhattan plots resulting from the meta-analysis of age-associated probes in FC (**A**), TC (**B**), ERC (**C**) and CRB (**D**). Significant aDMPs are marked with dark color. Scale change across 50 is indicated by an axis break.

Supplementary Figure 3. Manhattan plots of LOAD-DMPs in the four brain regions. The figure displays the Manhattan plots resulting from the meta-analysis of AD-associated probes in FC (**A**), TC (**B**), ERC (**C**) and CRB (**D**). Significant LOAD-DMPs are marked with dark color.

Supplementary file 1. Significant sDMPs in the four brain regions. The tables report the lists of sDMPs for each brain regions (FC, TC, ERC and CRB). Probes resulting from the analysis of cross-region and region-specific sDMPs are indicated by a cross, together with the probes that are in common with aDMPs or LOAD-DMPs found in the same region.

Supplementary file 2.Enrichment analysis of sDMPs. The tables report: 1) the results of Fisher's test on genomic distribution of sDMPs for each brain region, considering genomic context and chromosomal location. Significant results (p-value<0.05) are colored in green or red if depleted or enriched respectively. 2) the results of GO pathway enrichment analysis, after REVIGO filtering. Only the significant results (adjusted p-value <0.01) for each brain region are reported.

Supplementary file 3. Significant aDMPs in the four brain regions. The tables report the lists of aDMPs for each brain regions (FC, TC, ERC and CRB). Probes resulting from the analysis of cross-region and region-specific sDMPs are indicated by a cross, together with the probes that are in common with sDMPs or LOAD-DMPs found in the same region.

Supplementary file 4. Enrichment analysis of aDMPs. The tables report: 1) the results of Fisher's test on genomic distribution of aDMPs for each brain region, considering genomic context and chromosomal location. Significant results (p-value<0.05) are colored in green or red if depleted or enriched respectively. 2) the results of GO pathway enrichment analysis, after REVIGO filtering. Only the significant results (adjusted p-value <0.01) for each brain region are reported.

Supplementary file 5. Probes with significant sex-by-age interaction in the four brain regions. The tables report the lists of probes with significant sex-by-age interaction in each brain region (FC, TC, ERC and CRB).

Supplementary file 6. Significant LOAD-DMPs in the four brain regions. The tables report the lists of LOAD-DMPs for each brain regions (FC, TC, ERC and CRB). Probes resulting from the analysis of cross-region and region-specific LOAD-DMPs are indicated by a cross, together with the probes that are in common with sDMPs or aDMPs found in the same region.

Supplementary file 7.Enrichment analysis of LOAD-DMPs. The tables report: 1) the results of Fisher's test on genomic distribution of LOAD-DMPs for each brain region, considering genomic context and chromosomal location. Significant results (p-value<0.05) are colored in green or red if depleted or enriched respectively. 2) the results of GO pathway enrichment analysis, after REVIGO filtering. Only the significant results (adjusted p-value <0.01) for each brain region are reported.

Table 1. *Characteristics of the Infinium450kdatasets including healthy subjects selected in the present study for the age and sex analyses.*

Number of GEO accession	Regions	Number of subjects	Sex (F/M)	Age range
GSE105109	Entorhinal Cortex Cerebellum	27 28	13/14 14/14	58-99ys 58-99ys
GSE125895	Frontal Cortex Entorhinal Cortex	47 49	19/28 20/29	51.83-83.64ys 51.83-83.64ys
GSE134379	Temporal Cortex Cerebellum	179 179	76/103 76/103	63-103ys 63-103ys
GSE59685	Frontal Cortex Temporal Cortex Cerebellum	24 26 23	12/12 13/13 10/13	55-95ys 40-95ys 40-95ys
GSE74193	Frontal Cortex	216	68/148	19.26-85.2ys
GSE64509	Frontal Cortex Cerebellum	40 31	22/18 21/10	32-114ys 38-114ys
GSE66351	Frontal Cortex Temporal Cortex	25 25	10/15 10/15	46-88ys 46-88ys

Table 2. *Characteristics of the Infinium450kdatasets investigated in the present study including AD patients and non-demented control subjects.*

Number of GEO accession	Regions	Number of subjects	Sex (F/M)	Age range
GSE105109	Entorhinal Cortex **Ctrl** Entorhinal Cortex **AD** Cerebellum **Ctrl** Cerebellum **AD**	24 61 25 64	13/11 27/34 13/12 27/37	66-99ys 67-97ys 66-99ys 67-97ys
GSE125895	Frontal Cortex **Ctrl** Frontal Cortex **AD** Entorhinal Cortex **Ctrl** Entorhinal Cortex **AD** Cerebellum **Ctrl** Cerebellum **AD**	11 18 12 17 8 20	5/6 9/9 5/7 10/7 4/4 11/8	65.04-83.64ys 71.47-92.29ys 65.04-83.64ys 71.47-92.29ys 65.04-83.64ys 71.47-92.29ys
GSE134379	Temporal Cortex **Ctrl** Temporal Cortex **AD** Cerebellum **Ctrl** Cerebellum **AD**	175 217 175 217	76/99 117/100 74/95 117/100	68-103ys 66-102ys 68-103ys 66-102ys
GSE59685	Frontal Cortex **Ctrl** Frontal Cortex **AD** Temporal Cortex **Ctrl** Temporal Cortex **AD** Entorhinal Cortex **Ctrl** Entorhinal Cortex **AD** Cerebellum**Ctrl** Cerebellum**AD**	21 60 22 61 19 58 19 60	10/11 39/21 11/11 40/21 8/11 19/13 8/11 39/21	66-95ys 66-103ys 66-95ys 66-103ys 66-95ys 66-95ys 66-95ys 66-103ys
GSE66351	Frontal Cortex **Ctrl** Frontal Cortex **AD** Temporal Cortex **Ctrl** Temporal Cortex **AD**	12 35 12 37	8/4 22/13 8/4 23/14	71-88ys 67-97ys 71-88ys 67-97y
GSE76105	Temporal Cortex **Ctrl** Temporal Cortex **AD**	34 34	18/16 17/17	66-94ys 66-92ys

GSE80970	Frontal Cortex **Ctrl** Frontal Cortex **AD** Temporal Cortex **Ctrl** Temporal Cortex **AD**	68 74 70 74	34/34 54/30 36/34 54/30	70-108ys 72-103ys 70-108ys 72-103ys
GSE109627	Temporal Cortex **Ctrl** Temporal Cortex **AD**	36 46	19/17 24/22	73-94ys 70-95ys

Ctrl: non-demented control subjects; AD: Alzheimer's disease patients

Table 3. *List of sDMPs resulted from cross-region analysis.*

Probe	Chr	MAPINFO	Relation	Gene	Effect size direction	Yusipov et al.
cg00097357	12	33591336	N_Shore	SYT10	-	X
cg00655923	7	64895418			+	X
cg00760935	4	1.55E+08	Island	DCHS2	-	X
cg01063965	11	695461	Island	TMEM80, DEAF1	-	
cg01181499	2	74739419	N_Shore		-	X
cg01906879	3	81811016	S_Shore	GBE1	-	X
cg02093808	4	77342011	Island		-	X
cg02297043	1	75590912	Island		-	X
cg02530860	8	1.44E+08	Island		+	X
cg03168896	3	44036098	N_Shore		-	X
cg03405128	4	77341841	N_Shore		-	X
cg03687700	2	24271844	N_Shore	FKBP1B	-	X
cg03894796	8	1.44E+08	Island		+	X
cg04946709	16	59789030	Island	LOC644649	+	X
cg05020125	8	37605552		LOC728024, ERLIN2	-	X
cg05056638	8	24800824	S_Shore		-	X
cg05100634	18	45457604	Island	SMAD2	-	
cg05468028	21	30391383	Island	RWDD2B	-	X
cg05849319	11	65172370	Island	FRMD8	+	X
cg06666376	19	3480596	N_Shore	C19orf77	+	X
cg06710937	13	23489940	Island		-	X
cg07462804	4	81105375	Island	PRDM8	-	X
cg07645761	16	2892518	N_Shore	TMPRSS8	+	X
cg07953307	16	29000920		LAT	+	X
cg08541880	3	1.38E+08	Island	DZIP1L	-	X
cg09045105	1	1.5E+08	Island	BOLA1	-	X
cg09725915	2	70369583	Island		-	X
cg09971754	16	89557657	Island	ANKRD11	+	X
cg10546176	5	34929404	Island	DNAJC21	-	X
cg10749792	7	56119218	Island	PSPH, CCT6A	-	X
cg10776186	13	25875020	Island	NUPL1	-	X
cg11065518	2	2.08E+08	S_Shore	MDH1B, FASTKD2	-	X
cg11174255	4	1513259	N_Shore		+	X
cg11240062	8	1.44E+08	Island		+	X
cg11565911	12	72233249	N_Shore	TBC1D15	-	X
cg11841231	2	2.06E+08		PARD3B	+	X
cg12356266	8	99984350	N_Shore		-	X
cg12611527	2	1.57E+08	Island		-	X
cg12611723	9	1.4E+08	Island	NPDC1	-	X
cg13230424	17	45930033	S_Shore	SP6	-	X
cg13346869	8	37605517		LOC728024, ERLIN2	-	X
cg14030268	10	1.19E+08	Island	PDZD8	-	X
cg14373579	9	1.33E+08	Island	LOC100272217, FUBP3	-	X
cg15148078	19	3480561	N_Shore	C19orf77	+	X
cg15817705	1	2.09E+08	S_Shore		+	X
cg16021159	1	57142074		PRKAA2	+	X
cg16374663	15	41805031	Island	LTK	-	X
cg17561891	7	86849173	Island	C7orf23	-	X
cg17743279	7	92463268	Island	CDK6	-	X
cg17887478	17	7486551	Island	MPDU1	-	X
cg18001427	21	30391784	S_Shore	RWDD2B	-	X
cg18721420	19	15121913	Island	CCDC105	-	X
cg19292062	20	524344	Island	CSNK2A1	-	X

cg19311244	4	77341912	N_Shore		-	X
cg19864758	20	17206720	Island	PCSK2	-	X
cg20050113	2	1.03E+08	S_Shore	SLC9A2	-	X
cg20432211	4	77342104	Island		-	X
cg22105158	19	3480672	N_Shore	C19orf77	+	X
cg22266749	4	1.1E+08	Island	COL25A1	+	X
cg22345911	17	80231263	Island	CSNK1D	-	X
cg22794378	14	89029563	Island	ZC3H14	-	
cg22799420	14	1.02E+08	Island	DIO3	-	X
cg22889142	19	58862398	Island	NCRNA00181, A1BG	-	X
cg23001456	17	2615074	Island	KIAA0664	-	X
cg23719534	15	1.01E+08	Island		-	
cg23880736	4	582172	Island		+	X
cg24016844	1	1.12E+08	Island	C1orf103	+	X
cg24126849	4	581937	N_Shore		+	X
cg24158363	17	73401717	Island	GRB2	-	X
cg24717799	15	83680832	S_Shore	C15orf40	-	X
cg24990494	13	32520050		EEF1DP3	+	
cg25584814	19	345306	Island	MIER2	-	X
cg25726513	4	1340596	Island	KIAA1530	-	X
cg26172013	20	32031452	Island	SNTA1	-	X
cg26516287	7	12629275		SCIN	-	X
cg26612727	17	38024636	Island	ZPBP2	-	X
cg27645294	17	21795257			-	X

Table 4. *List of aDMPs resulting from cross-region*

Probe	Chr	MAPINFO	Relation	Gene	Effect size direction	Yusipov et al.
cg00292135	7	156433068	Island	C7orf13, RNF32	+	X
cg04090392	15	83952774	Island	BNC1	+	X
cg06639320	2	106015739	Island	FHL2	+	X
cg06942814	7	27170819	S_Shore	HOXA4	+	X
cg07303143	3	44803452	Island	KIAA1143;KIF15	+	X
cg07525420	10	131761181	Island	EBF3	+	X
cg07922606	6	26225389	Island	HIST1H3E	+	
cg11614451	3	160167729	Island	TRIM59	+	
cg12373771	22	17601381	Island	CECR6	+	X
cg13327545	10	22623548	Island		+	X
cg14020846	14	103674272	Island		+	X
cg14556683	19	15342982	Island	EPHX3	+	X
cg15243034	11	77907656	Island	USP35	+	X
cg15341124	14	102027734	Island	DIO3, MIR1247	+	X
cg15611336	15	75248496	Island	RPP25	+	X
cg16295725	4	10459219	Island	ZNF518B	+	X
cg16867657	6	11044877	Island	ELOVL2	+	X
cg16969368	17	57642752	Island	DHX40	+	X
cg18008766	2	38978896	S_Shore	SFRS7	+	X
cg18240400	10	46168597	Island	ANUBL1	+	X
cg18473521	12	54448265	S_Shore	HOXC4	+	X
cg19399220	19	10527588	Island		+	X
cg20591472	1	110008990	Island	SYPL2	+	X
cg23995914	4	10459228	Island	ZNF518B	+	X
cg24079702	2	106015771	Island	FHL2	+	X
cg24567591	16	3931229	Island	CREBBP	+	X
cg24903144	10	102509268	Island	PAX2	+	X
cg26092675	6	26225258	N_Shore	HIST1H3E	+	X

Table 5. *List of LOAD-DMPs resulting from cross-region analysis.*

Intersection	Probe	Chr	MAPINFO	Relation	Gene	Effect size direction	Smith et al. (Bonf. Corrected sDMPs)
TC ∩ERC	cg00851830	14	100201016	N_Shelf		+	
	cg03169557	16	89598950		SPG7	+	X
	cg03183618	2	134964228			+	
	cg04658038	17	64800166		PRKCA	+	
	cg05066959	8	41519308		ANK1, MIR486	+	X
	cg05397697	14	90042217		PRO1768, FOXN3	+	
	cg05417607	17	1373605	N_Shore	MYO1C	+	X
	cg05810363	17	74475270	Island	RHBDF2	+	X
	cg06653632	12	129281444	S_Shore	SLC15A4	+	
	cg06753513	17	3977385		ZZEF1	+	
	cg07012687	17	80195180	Island	SLC16A3	+	
	cg07571519	10	73472315		C10orf105	+	
	cg09123026	17	74480528		RHBDF2	+	
	cg11823178	8	41519399		ANK1, MIR486	+	X
	cg12163800	17	74475355	Island	RHBDF2	+	X
	cg12309456	17	74475402	Island	RHBDF2	+	X
	cg13851211	16	50321678		ADCY7	+	
	cg14025831	20	3873404	S_Shelf	PANK2	+	
	cg14761246	3	182968758	N_Shelf	MCF2L2	+	
	cg14798745	4	184315677	N_Shelf		+	
	cg18102633	19	17487776	N_Shore	PLVAP	+	
	cg18456331	10	77188318	N_Shelf		+	
	cg18923906	10	82225771		TSPAN14	+	
	cg20148994	7	130125585	N_Shore	MEST	+	
	cg21221455	15	63342288	S_Shore	TPM1	+	
	cg22090150	17	4098227		ANKFY1	+	X
	cg22656126	17	1637206	Island	WDR81	+	
	cg25018458	17	980014	N_Shore	ABR	+	X
FC ∩TC ∩ERC	cg27630153	16	88845038	Island	FAM38A	+	
	cg12163800	17	74475355	Island	RHBDF2	+	X
FC ∩TC	cg01463828	8	22446721		PDLIM2	+	X
	cg02317313	12	1,22E+08	Island	LOC338799	+	X
	cg04874795	16	86477638			-	X
	cg07061298	7	27153847	N_Shore	HOXA3;	+	X
	cg12163800	17	74475355	Island	RHBDF2	+	X
	cg22962123	7	27153605	Island	HOXA3	+	X
	cg26022064	7	98739782	N_Shore	SMURF1	+	X
FC ∩ ERC	cg26199857	12	54764265	Island	ZNF385A	+	
	cg12163800	17	74475355	Island	RHBDF2	+	X
	cg13076843	17	74475294	Island	RHBDF2	+	X

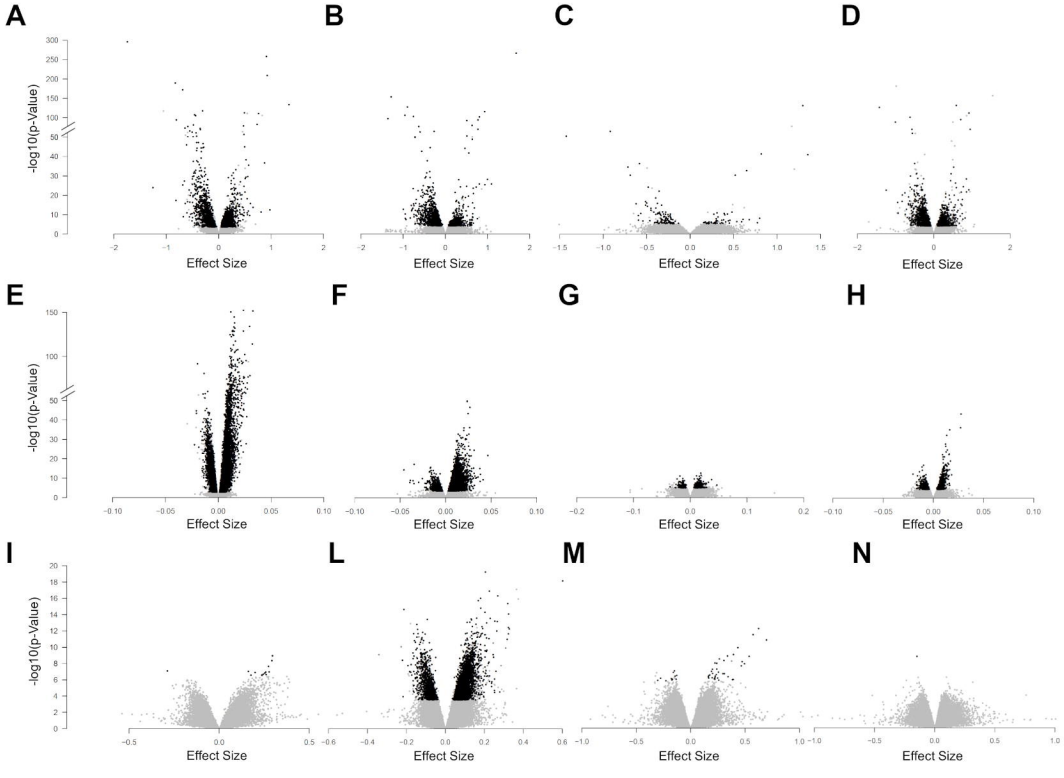
A
B
C
D
E
F
G
H
I
L
M
N
-log10(p-Value)
Effect Size

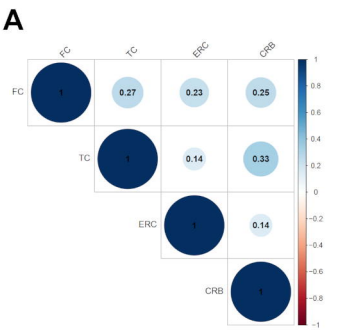

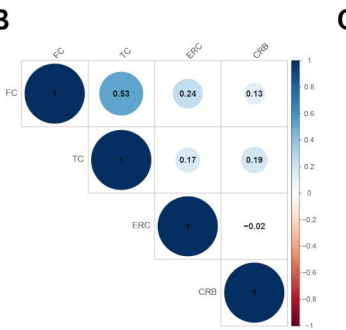

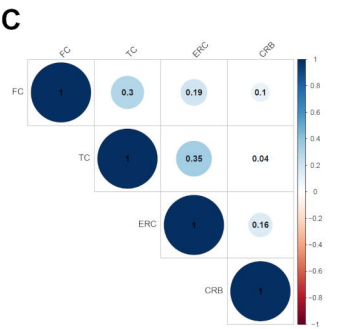

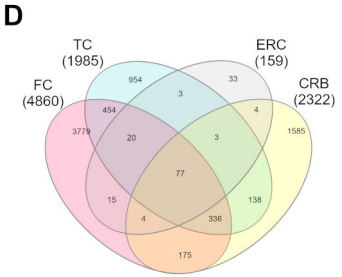

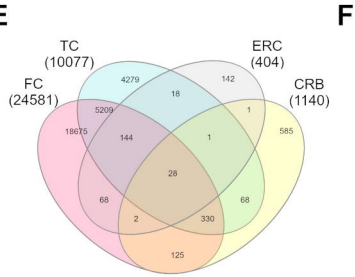

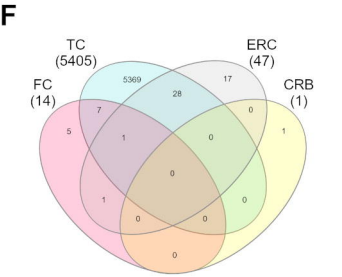

FC ∩ TC ∩ ERC ∩ CRB:

A1BG
ANKRD11
BOLA1
C15orf40
C19orf77
C1orf103
C7orf23
CCDC105
CCT6A
CDK6
COL25A1
CSNK1D
CSNK2A1
DCHS2
DEAF1
DIO3
DNAJC21
DZIP1L
EEF1DP3
ERLIN2
FASTKD2
FKBP1B
FRMD8
FUBP3
GBE1
GRB2
KIAA0664
KIAA1530
LAT
LOC100272217
LOC644649
LOC728024
LTK
MDH1B
MIER2
MPDU1
NCRNA00181
NPDC1
NUPL1
PARD3B
PCSK2
PDZD8
PRDM8
PRKAA2
PSPH
RWDD2B
SCIN
SLC9A2
SMAD2
SNTA1
SP6
SYT10
TBC1D15
TMEM80
TMPRSS8
ZC3H14
ZPBP2

FC ∩ TC ∩ ERC ∩ CRB:

ANUBL1
BNC1
C7orf13
CECR6
CREBBP
DHX40
DIO3
EBF3
ELOVL2
EPHX3
FHL2
MIR1247
HIST1H3E
RNF32
HOXA4
HOXC4
KIAA1143
PAX2
RPP25
SFRS7
SYPL2
TRIM59
USP35
ZNF518B
KIF15

FC ∩ TC ∩ ERC:

RHBDF2

FC ∩ ERC:

RHBDF2

FC ∩ TC:

HOXA3
SMURF1
PDLIM2
LOC338799
RHBDF2
ZNF-385A

TC ∩ ERC:

ABR
ADCY7
ANK1
ANKFY1
C10orf105
CDH23
FAM38A
FOXN3
MCF2L2
MEST
MIR486
MYO1C
PANK2
PRKCA
PRO1768
RHBDF2
SLC15A4
SLC16A3
SPG7
TPM1
TSPAN14
WDR81
ZZEF1

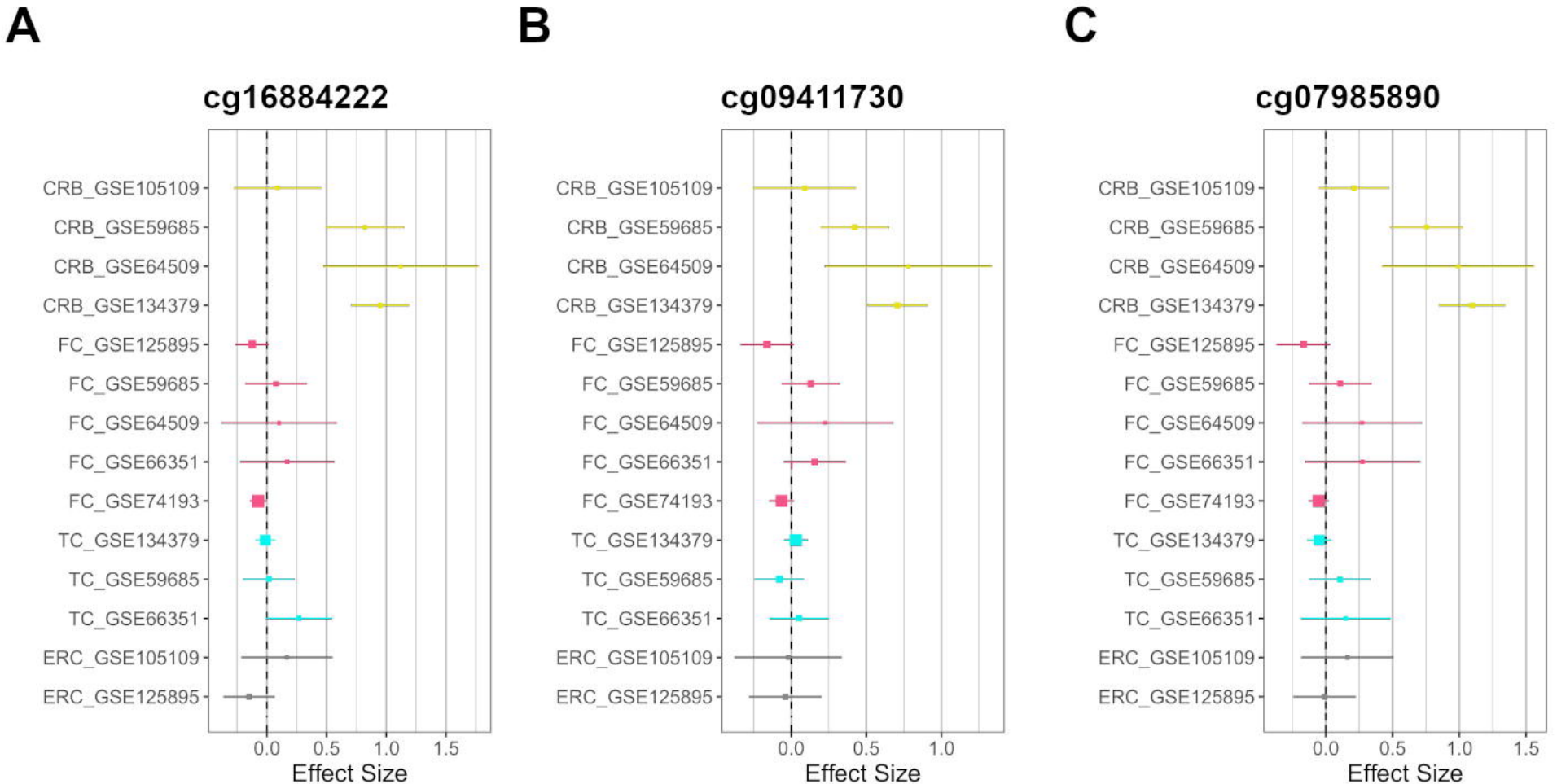
A
cg16884222
CRB_GSE105109
CRB_GSE59685
CRB_GSE64509
CRB_GSE134379
FC_GSE125895
FC_GSE59685
FC_GSE64509
FC_GSE66351
FC_GSE74193
TC_GSE134379
TC_GSE59685
TC_GSE66351
ERC_GSE105109
ERC_GSE125895
0.0
0.5
1.0
1.5
Effect Size
B
cg09411730
CRB_GSE105109
CRB_GSE59685
CRB_GSE64509
CRB_GSE134379
FC_GSE125895
FC_GSE59685
FC_GSE64509
FC_GSE66351
FC_GSE74193
TC_GSE134379
TC_GSE59685
TC_GSE66351
ERC_GSE105109
ERC_GSE125895
0.0
0.5
1.0
Effect Size
C
cg07985890
CRB_GSE105109
CRB_GSE59685
CRB_GSE64509
CRB_GSE134379
FC_GSE125895
FC_GSE59685
FC_GSE64509
FC_GSE66351
FC_GSE74193
TC_GSE134379
TC_GSE59685
TC_GSE66351
ERC_GSE105109
ERC_GSE125895
0.0
0.5
1.0
1.5
Effect Size

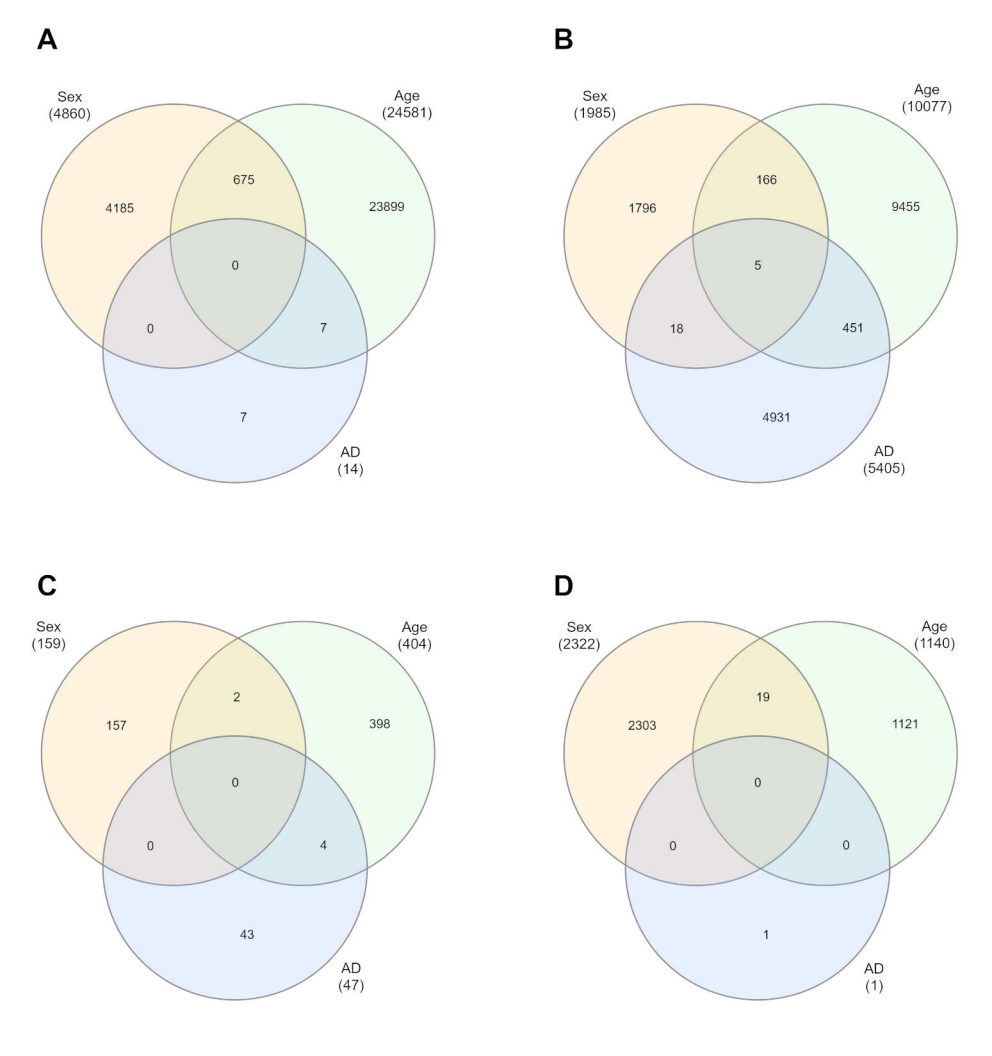
A
Sex
(4860)
Age
(24581)
AD
(14)
4185
675
23899
0
0
7
7
B
Sex
(1985)
Age
(10077)
AD
(5405)
1796
166
9455
5
18
451
4931
C
Sex
(159)
Age
(404)
AD
(47)
157
2
398
0
0
4
43
D
Sex
(2322)
Age
(1140)
AD
(1)
2303
19
1121
0
0
0
1

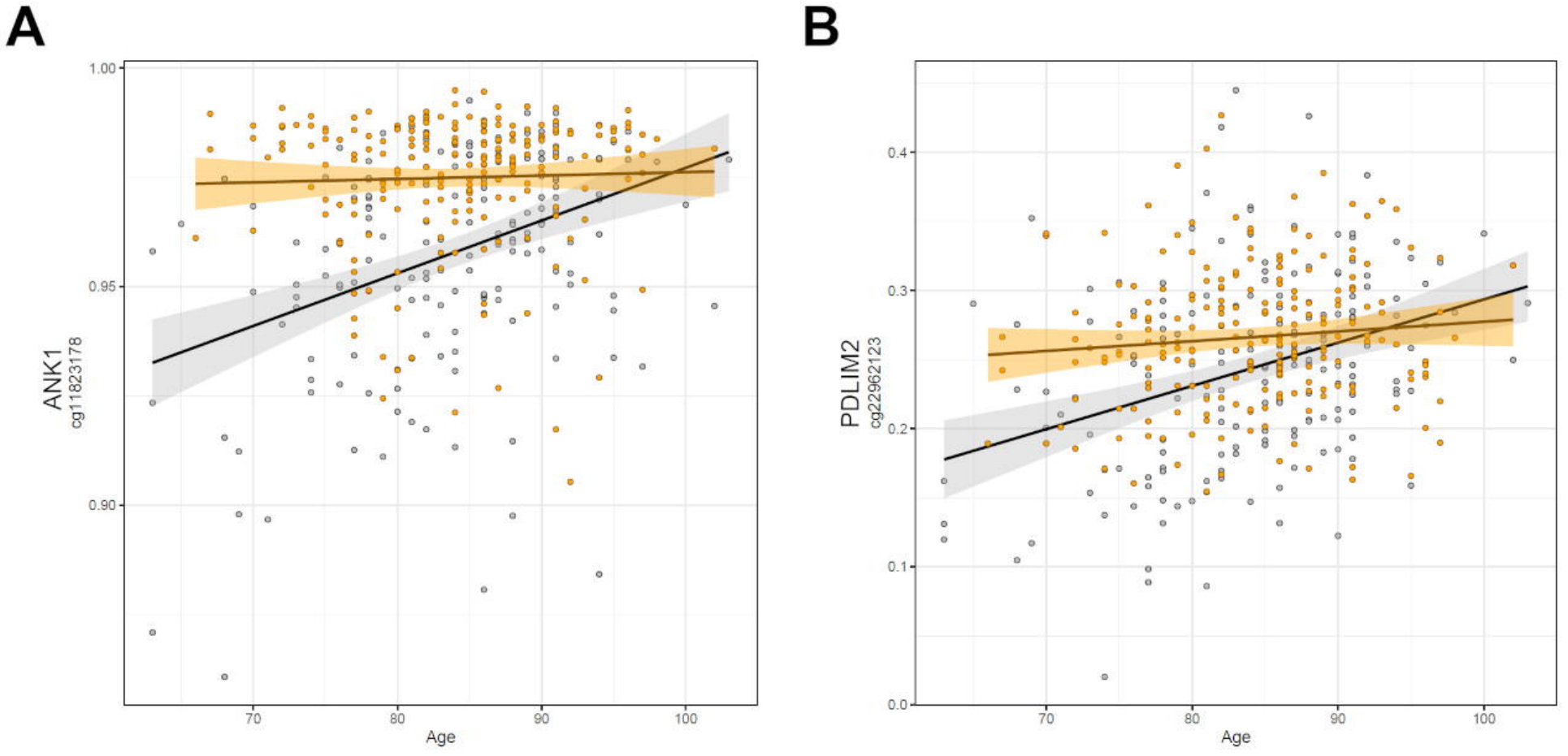
A
ANK1
cg11823178
1.00
0.95
0.90
70
80
90
100
Age
B
PDLIM2
cg22962123
0.4
0.3
0.2
0.1
0.0
70
80
90
100
Age